Proteomics comparison between mass-like and non-mass-like breast lesions

Shi-Yu Li[1], Bo Wang[1], Ying Jiang[1], Junkang Li[1], Gang Liu[2], Zhi-Li Wang[1]

[1]Department of Ultrasound, The First Medical Center of PLA General Hospital, Beijing, China; [2]Department of Radiology, The First Medical Center of PLA General Hospital, Beijing, China

Contributions: (I) Conception and design: SY Li, ZL Wang; (II) Administrative support: G Liu, ZL Wang; (III) Provision of study materials or patients: SY Li, B Wang; (IV) Collection and assembly of data: Y Jiang, J Li; (V) Data analysis and interpretation: SY Li, J Li; (VI) Manuscript writing: All authors; (VII) Final approval of manuscript: All authors.

Correspondence to: Gang Liu. Department of Radiology, The First Medical Center of PLA General Hospital, 28 Fuxing Road, Beijing 100853, China. Email: lgwzl@126.com; Zhi-Li Wang, MD. Department of Ultrasound, The First Medical Center of PLA General Hospital, 28 Fuxing Road, Beijing 100853, China. Email: wzllg@sina.com.

Background: The proteomic differences between mass-like (ML) breast lesions and non-mass-like (NML) breast lesions were compared to explore the formation mechanism of NML ultrasonic morphological characteristics.

Methods: From January to August 2021, tissue samples were collected from 10 patients with malignant ML (MML), 10 patients with malignant NML (MNML), 10 patients with benign ML (BML), and seven patients with benign NML (BNML). The proteomic differences between the BML and BNML groups and the MML and MNML groups were compared by data-independent acquisition (DIA) quantitative mass spectrometry. The differentially expressed proteins were analyzed by Gene Ontology (GO), Kyoto Encyclopedia of Genes and Genomes (KEGG), and protein-protein interaction (PPI) networks analyses.

Results: We identified a total of 623 significantly differentially expressed proteins in the MML/MNML group, and 167 significantly differentially expressed proteins in the BML/BNML group, with relative ratios >1.2 or <–0.83. The up-regulated differential proteins were more abundant in the tumor necrosis factor (TNF) signaling pathway in both the MML/MNML and BML/BNML groups, suggesting that the TNF signaling pathway may be related to the ultrasonic morphological characteristics of breast lesions. Dual specificity mitogen-activated protein kinase 3 (MP2K3), a protein factor in the TNF signaling pathway, exhibited significant upregulation in both the malignant and BML groups.

Conclusions: The TNF signaling pathway may be associated with the ultrasonic morphological characteristics of breast lesions. MP2K3 is the up-regulated differential expression protein in the MML/MNML and BML/BNML groups, which may be related to the ultrasonic morphological characteristics of breast lesions.

Keywords: Breast lesions; non-mass breast lesions; proteomics

Introduction

Breast cancer is the most common malignant tumor and the second most common cause of cancer-related death in women (1). Although the overall 5-year survival rate has improved, at least 20 % of patients continue to develop metastatic disease, with a poor prognosis (2). At present, histopathological factors including tumor size, grade, lymph node status, hormone, and human epidermal growth factor receptor-2 (HER2) receptor status can be used to guide breast cancer treatment and predict prognosis (3). However,

the prognosis of many patients with histologically similar tumors may be very different, so additional biomarkers for prediction, diagnosis, and prognosis are still needed.

Since the results of conventional ultrasound (US) are not affected by breast density, US has become a routine imaging tool for breast detection and diagnosis (4). According to the Breast Imaging Reporting and Data System (BI-RADS)-US released by the American College of Radiology, mass-like (ML) lesions are those that exhibit a mass effect on two different planes (5). However, 5–9 % of breast lesions present as localized asymmetric focal low echo areas on two vertical planes with no apparent margin or shape, and therefore do not meet the strict "mass" criteria defined by BI-RADS (6). Radiologists refer to these as non-mass-like (NML) lesions, which correspond to non-mass enhancement on breast magnetic resonance imaging (7).

The histological presentation of NML breast cancer tends to be ductal component-dominant ductal carcinoma in situ (DCIS) and invasive ductal carcinoma (8,9). Previous studies have shown that the ultrasonographic appearance of breast cancer as mass or non-mass may be related to the adequacy of nutrition (10,11). Franks *et al.* (11) used the nutritional restriction model to describe tumor growth, obtained nutrients by diffusion from the surroundings, and determined the birth and death of breast cancer cells by the concentration of nutrients. Their results showed that breast cancer with sufficient nutrition was more invasive and prone to ML growth. When nutrition is insufficient, breast cancer tends to grow along the ducts, presenting as NML.

Highlight box

Key findings
- MP2K3 is the up-regulated differential expression protein in the MML/MNML and BML/BNML groups, which may be related to the ultrasonic morphological characteristics of breast lesions.

What is known and what is new?
- Current studies have shown that proteomics is significantly different in different types of breast cancer and between breast cancer and adjacent normal tissues.
- In this study, the proteomics of mass-like and non-mass-like breast lesions was significantly different. The tumor necrosis factor signaling pathway may be associated with the ultrasonic morphological characteristics of breast lesions.

What is the implication, and what should change now?
- Further exploration of the specific mechanism of the tumor necrosis factor signaling pathway in the formation of malignant ML and NML ultrasonic morphology is needed.

Ko *et al.* (12) explored the morphological characteristics of triple-negative breast cancer [estrogen receptor (ER)/progesterone receptor (PR)/human epidermal growth factor receptor 2 (HER2) negative] and found that 86% of triple-negative breast cancer exists in the form of mass, and is less manifested as non-mass lesions. Jiang *et al.* (13) showed that there was only a significant difference in histological grades between mass type and malignant NML (MNML), while those of ER, PR, HER2, P53, and Ki-67 did not exhibit significant differences. Therefore, further study is still needed on the formation mechanism of the morphological features of ML and NML US images.

Data-independent acquisition (DIA) is a major advance in protein quantification, enabling high-throughput quantitative proteomics (14). With the help of spectral libraries from previous DIA experiments or auxiliary data-dependent acquisition (DDA) data, DIA analysis can obtain the same repeatability and accuracy as parallel reaction monitoring (PRM) identification and quantification, except for low-abundance peptides that are blocked by strong signals (15). Non-targeted DIA has shown great potential in comprehensively revealing and validating the predictive and prognostic candidate biomarkers for various diseases, such as cancer, liver failure, and breast cancer (16). Numerous studies have shown that the screening of breast cancer proteomics information plays an important role in the classification of functional subtypes and staging of breast cancer, revealing the mechanism of breast cancer, and exploring the metastatic and invasive properties of breast cancer (17,18). In addition, some studies have shown that proteomics can also be applied for the prediction of breast cancer recurrence, the assessment and reduction of cancer cell resistance, and the selection and monitoring of the most appropriate breast cancer treatment programs as well as other prognostic and therapeutic studies (19,20).

At present, further study on the formation mechanism of the morphological characteristics of ML and NML US images, especially malignant ML (MML) and NML, is still needed. In this study, the DIA method was employed to detect the differences between ML and NML proteomics, aiming to explore the formation mechanism of the morphological characteristics of ML and NML US images. Our findings provide a basis for the pathological study of the morphological characteristics of ML and NML in US images of breast lesions. We present the following article in accordance with the MDAR reporting checklist (available at https://atm.amegroups.com/article/view/10.21037/atm-22-6655/rc).

Methods

Patients

The experimental samples were derived from 42 cases of ML and NML breast lesions treated by vacuum-assisted breast biopsy or tumor resection in the US diagnosis and general surgery departments of our hospital from January to August 2021, including 10 cases of MML, 10 cases of benign ML (BML), 10 cases of MNML, and seven cases of benign NML (tissue size: 300–500 mg per case).

The patients included in the study were 18–70-year-old women whose conventional breast US examinations showed ML and NML. Also, the pathological results of the patients were clear, and all patients signed the informed consent. This study was approved by the ethics committee of the First Medical Center of PLA General Hospital (No. S2021-683-01). The study was conducted in accordance with the Declaration of Helsinki (as revised in 2013).

Sample collection

During vacuum-assisted breast biopsy and treatment, benign NML or ML lesion tissues were taken directly. After breast cancer was confirmed by frozen section pathology, MNML or ML tumor tissues and adjacent tissues were collected directly during tumor resection in breast surgery, and the proportion of non-necrotic tumor tissues was >70%. The tissue size was 300–500 mg. The specimens were placed in a labeled frozen tube and quickly frozen in liquid nitrogen. The specimens were then stored in a refrigerator at –80 ℃ within 20 minutes.

Protein extraction and enzymolysis

The samples were chopped with liquid nitrogen, lysed in lysis buffer containing 50 mM ammonium bicarbonate (NH4HCO3) pH 7.4, 10 mM magnesium chloride (MgCl$_2$), 7 M urea, and 2 M thiourea, and then sonicated on ice for 5 min. The lysate was then centrifuged at 12,000 g at 4 ℃ for 15 min, and the supernatant was transferred to a clean tube. The protein concentration was determined using a Bradford protein assay. Each sample was reduced with 10 mM dithiothreitol (DTT) at 56 ℃ for 1 h and then alkylated with enough iodoacetamide in the dark at room temperature for 1 h. The protein was digested with trypsin (Promega, Beijing) at a substrate ratio of 1:50. After digestion at 37 ℃ for 16 h, some peptides in the sample were uniformly mixed. The digestion solution was lyophilized and the peptide was redissolved with 25 mM NH4HCO3 30 µL per tube.

High-performance liquid chromatographic separation

A C18 column (Waters BEH, China, C18 4.6×250 mm, 5 µm) and Rigol (China) L3000 HPLC column were used. The column temperature was 50 ℃, and the mobile phases A (2% acetonitrile, adjusted pH to 10.0 with ammonium hydroxide) and B (98% acetonitrile, adjusted pH to 10.0 with ammonium hydroxide) were applied. Ammonium hydroxide regulated pH to 10.0 gradient elution. The solvent gradient was as follows: 3% B, 5 min; 3–8% B, 0.1 min; 8–18% B, 11.9 min; 18–32% B, 11 min; 32–45% B, 7 min; 45–80% B, 3 min; 80% B, 5 min; and 80–5%, 0.1 min, 5% B, 6.9 min. The eluent was monitored at UV214 nm and collected at a rate of one tube per minute. Finally, six components were synthesized and all components were dried under vacuum and reconstituted in 0.1% (v/v) formic acid (FA) water. 0.2 µL of standard peptide was added to the distilled sample for subsequent analysis.

Liquid chromatography-mass spectrometry/mass spectrometry (LC-MS/MS) analysis—DDA mode

Proteomics analysis was performed using a U3000 UHPLC system (Thermo Fisher, Beijing) and an Orbitrap fusion mass spectrometer (Thermo Fisher, Beijing) in DDA mode. A total of 1 µg of total peptide was extracted from the sample extracted with 0.1 % formic acid (FA) and injected into a self-made C18 Nano-Trap column (2 cm × 100 µm, 3 µm). The analytical column (25 cm × 75 µm, 100 A) was used to separate the peptides. The eluent B (0.08 % FA in 80% acetonitrile (ACN), 20 % water) and eluent A (0.1% FA) were linearly graded in the range of 0–100 % for 120 min at a flow rate of 350 nL/min. The detailed solvent gradient was as follows: 0–4% B, 8 min; 4–10% B, 11 min; 10–25% B, 88 min; 25–50% B, 98 min; 50–99% B, 102 min; 99–0% B.

LC-MS/MS analysis—DIA mode

A 100 mg sample was reconstituted in 0.1% FA, mixed with 0.2 µL standard peptide [indexed retention time, (IRT) kit, Biognosys, Beijing], and entered into a U3000U HPLC system (Thermo Fisher) for DIA using an Orbitrap fusion mass spectrometer (Thermo Fisher). The liquid phase conditions were the same as those used for DDA. For DIA acquisition, the an intact (ms1) resolution was set to 120,000

Page 4 of 12

Li et al. Proteomic comparison of breast ML and NML lesions

Table 1 Sample protein concentration

Sample name	Concentration (µg/µL)	Volume (µL)	Overall amount (µg)	Sample level
A1	1.62	700	1,134.89	A1
A2	4.43	700	3,099.89	A1
A3	8.92	700	6,240.85	A1
A4	2.10	500	1,049.58	A1
A5	1.16	500	579.76	A1
A6	3.14	700	2,197.65	A1
A7	6.38	700	4,467.97	A1
A8	3.49	700	2,444.32	A1
A9	1.19	700	829.52	A1
A10	3.72	700	2,603.40	A1
B1	1.89	700	1,321.37	A1
B2	4.52	700	3,167.44	A1
B3	3.45	700	2,417.43	A1
B4	4.60	700	3,223.26	A1
B5	2.55	700	1,786.52	A1
B6	1.06	700	742.52	A1
B7	1.11	700	776.64	A1
B8	1.90	700	1,333.06	A1
B9	0.93	700	648.11	A1
B10	1.90	700	1,333.06	A1
C1	1.43	700	1,000.26	A1
C2	2.81	700	1,969.56	A1
C3	1.40	700	980.39	A1
C4	2.53	700	1,768.28	A1
C5	3.48	700	2,438.93	A1
C6	1.83	700	1,282.83	A1
C7	1.58	700	1,106.50	A1
C8	7.90	700	5,528.30	A1
C9	2.72	500	1,359.11	A1
C10	1.72	500	859.94	A1
D1	1.84	700	1,290.49	A1
D2	1.24	700	868.96	A1
D3	1.02	700	714.76	A1
D4	2.46	700	1,718.64	A1
D5	2.08	700	1,457.08	A1
D6	1.11	700	779.53	A1
D7	2.54	700	1,777.39	A1

and the fragmented (ms2) resolution was set to 30,000. The M/z range was 350–1,350 m/z with a variable of 60 cycles. The full scan automatic gain control (AGC) target was set at 4×10^6, and the injection time was 50 ms. DIA was set to 35% normalized collision energy (NCE) with a target value of 1×10^6 and a maximum injection time AUTO to enable the mass spectrometer to always operate in parallel ion filling and detection mode.

LC-MS/MS DIA data analysis

For different comparison groups, the fold change (FC) and P value of each comparison method were analyzed and calculated, and the differential proteins were screened according to the following screening rules: FC >1.2 or FC <1/1.2, P<0.05. The differences were listed in tables, and a volcano map was created using the Msstats R package.

Using the Homo sapiens database, Gene Ontology (GO), Kyoto Encyclopedia of Genes and Genomes (KEGG), and protein-protein interaction (PPI) networks analyses were performed to summarize and explain the functional localization and metabolic pathways of differentially expressed proteins in MML and MNML and BML and benign NML (BNML).

Results

Analysis of the protein concentration of all samples

Before DIA proteomics quantitative detection of NML and ML, we measured the sample tissue and extracted the protein concentration. The results are shown in *Table 1*. The tissue proteins of each sample reached the A1 standard, that is, the gel map was clear, the bands were rich, and there was no high abundance. Furthermore, 10 µg of each sample was taken for sodium dodecyl sulfate polyacrylamide gel electroph (SDS-PAGE). The electrophoretic band is good and meets the requirements of the experiment, so the follow-up analysis can be continued.

Functional categorization/classification and pathway analysis of differentially expressed proteins

The study subjects were divided into two comparison groups: MML/MNML and BML/BNML. MML/MNML compared the protein expression profiles of 10 pairs of MML and MNML, and the BML/BNML group compared the protein expression profiles of 10 benign mass breast

lesions and seven benign non-mass breast lesions.

The DIA technique was used to quantify the proteins in the two comparison groups (FC >1.2 or FC <1/1.2, and P<0.05). In the MML/MNML group, there were 623 differentially expressed proteins, including 463 up-regulated proteins and 160 down-regulated proteins, such as Transforming growth factor beta 1 (TGF-β1), thrombospondin-1 (TSP1), Integrin Subunit Beta 5(ITGB5), insulin-like growth factors (IGF1), dual specificity mitogen-activated protein kinase kinase 3 (MP2K3), and other proteins, which may be related to the formation of MML. In the BML/BNML group, there were 167 differentially expressed proteins, of which 78 were up-regulated and 89 were down-regulated (Table 2). Figure 1 shows a volcano plot of these proteins. The protein with statistically significant difference (FC >1.2 or FC <1/1.2, and P<0.05) was located in the upper right and upper left quadrants. The top 10 up-regulated and down-regulated proteins in the MML/MNML and BML/BNML groups are shown in Tables 3-6.

To further explore the molecular biological functions of the differentially expressed proteins, we performed GO analysis on the differentially expressed proteins in each group. Taking P=0.05 as the critical value, Fisher's exact test was used to evaluate the significance level of protein enrichment in the GO entries. The top 10 proteins in terms of biological process (BC), cellular component (CC), and molecular function (MF) of MML/MNML (Figure 2A) and BML/BNML (Figure 2B) groups were listed. In the MML/MNML group, differential proteins were primarily expressed in the proteasome, cytoplasm, and cell membrane, mainly playing a role in vesicle-mediated transport, the immune system process, and the protein transport cell cycle, and participating in tumor immunity and transcription. In the BML/BNML group, the differential proteins were primarily expressed in ribosomes, lysosomes, and mitochondria, mainly playing a role in the combination of compounds, proteins, and DNA, and participating in carbohydrate metabolism.

In the MML/MNML group, 38 of the 271 pathways that up-regulated differential protein enrichment were statistically significant (P<0.05). Among the 123 pathways that down-regulated differential protein enrichment, 10 were statistically significant (P<0.05). The results of the BML/BNML group showed that 12 out of 138 pathways up-regulated differential protein enrichment were statistically significant (P<0.05). Among the 216 pathways

Table 2 Differential protein statistics

Comparisons	Up-	Down-	All-
MML/MNML	463	160	623
BML/BNML	78	89	167

MML, malignant mass-like; MNML, malignant non-mass-like; BML, benign mass-like; BNML, benign non-mass-like.
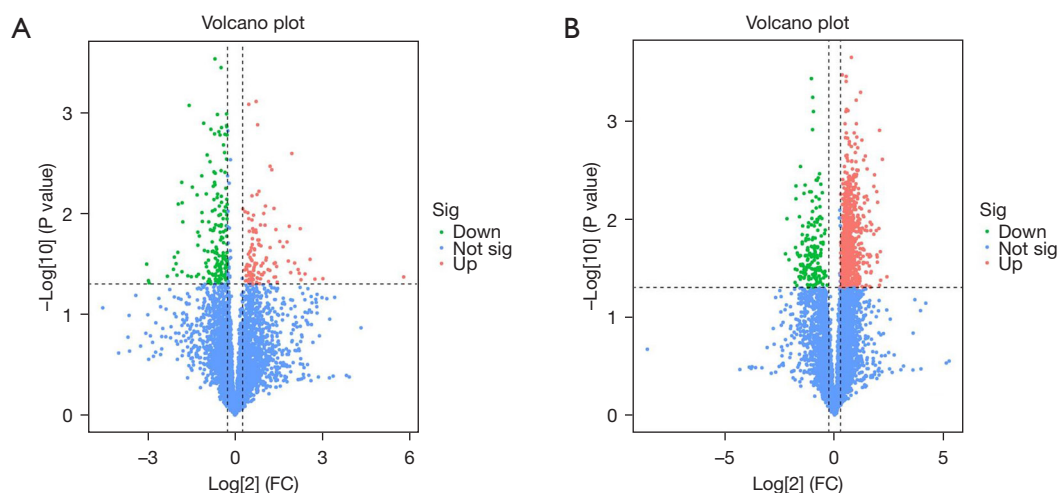

Figure 1 Quantitative volcano plot of differentially expressed proteins in each group. (A) The quantitative volcano plot of differentially expressed proteins in the MML/MNML group; (B) the quantitative volcano plot of differentially expressed proteins in the BML/BNML group. FC, fold change; MML, malignant mass-like; MNML, malignant non-mass-like; BML, benign mass-like; BNML, benign non-mass-like.

Page 6 of 12

Li et al. Proteomic comparison of breast ML and NML lesions

Table 3 Some up-regulated proteins in MML/MNML

ID	Gene name	Description	FC	P value
EXOS8	EXOSC8	Exosome complex component RRP43	5.239119	0.038737
RAD1	RAD1	Cell cycle checkpoint protein RAD1	4.560509	0.002449
BAK	BAK1	Bcl-2 homologous antagonist/killer	4.309771	0.042191
RENR	ATP6AP2	Renin receptor	4.265214	0.021494
MDN1	MDN1	Midasin	4.166939	0.001236
PAF1	PAF1	RNA polymerase II-associated factor 1 homolog	4.161053	0.047368
CD53	CD53	Leukocyte surface antigen CD53	4.079058	0.012453
RM47	MRPL47	39S ribosomal protein L47, mitochondrial	3.894424	0.006753
PUS7	PUS7	Pseudouridylate synthase 7 homolog	3.872687	0.027459
HLAH	HLA-H	Putative HLA class I histocompatibility antigen, alpha chain H	3.847482	0.024387

MML, malignant mass-like; MNML, malignant non-mass-like; FC, fold change; HLA, human leukocyte antigen.

Table 4 Some down-regulated proteins in MML/MNML

ID	Gene name	Description	FC	P value
ATD3B	ATAD3B	ATPase family AAA domain-containing protein 3B	0.210834	0.022599
KREM	KREMEN2	Kremen protein 2	0.220546	0.009884
APOF	APOF	Apolipoprotein F	0.234497	0.025941
TSH3	TSHZ3	Teashirt homolog 3	0.285312	0.044328
ABCC8	ABCC8	ATP-binding cassette sub-family C member 8	0.287352	0.032497
HPT	HP	Haptoglobin	0.28974	0.019481
TTHY	TTR	Transthyretin	0.293492	0.004586
CBPB1	CPB1	Carboxypeptidase B	0.293832	0.006205
BBS7	BBS7	Bardet-Biedl syndrome 7 protein	0.302366	0.047709
UT14C	UTP14C	U3 small nucleolar RNA-associated protein 14 homolog C	0.304547	0.032968

MML, malignant mass-like; MNML, malignant non-mass-like; FC, fold change; AAA, ATPase associated with various cellular activities.

that down-regulated differential protein enrichment, 15 were statistically significant (P<0.05). The top 10 up-and down-regulated protein enrichment results in the MML/MNML (*Figure 3A,3B*) and BML/BNML (*Figure 3C,3D*) groups are shown. The up-regulated differential proteins were significantly enriched in the tumor necrosis factor (TNF) signaling pathway in both the MML/MNML and BML/BNML groups, suggesting that the TNF signaling pathway may have a certain correlation with the ultrasonic morphological characteristics of breast lesions.

The results also showed that the expressions of KS6A5, NFKB1, CASP3, MK09, MP2K4, MP2K3, MP2K6,

FADD, CASP8, MLKL, and PGAM5 were up-regulated in the MML/MNML group. In the BML/BNML group, the expressions of MMP9, TNR6, and MP2K3 were up-regulated. The expression of MP2K3 was up-regulated in both MML/MNML and BML/BNML groups. The String database was used to analyze the differential proteins in the MML/MNML and BML/BNML groups, and a PPI network was constructed to explore the interaction between differential proteins. According to the degree of connectivity, the key proteins of the top 10 differentially expressed proteins in the MML/MNML and BML/BNML groups were screened out. The specific connection results

Table 5 Some up-regulated proteins in BML/BNML

ID	Gene name	Description	FC	P value
BAHC1	BAHCC1	BAH and coiled-coil domain-containing protein 1	55.62595	0.042654
PLF4	PF4	Platelet factor 4	8.1197	0.044365
NGRN	NGRN	Neugrin	6.70711	0.044657
ITA2B	ITGA2B	Integrin alpha-IIb	5.987456	0.028433
CXCL7	PPBP	Platelet basic protein	5.318866	0.039697
HBD	HBD	Hemoglobin subunit delta	4.802102	0.045545
ITB3	ITGB3	Integrin beta-3	4.74663	0.014112
HBB	HBB	Hemoglobin subunit beta	4.624392	0.039199
ANCHR	ZFYVE19	Abscission/NoCut checkpoint regulator	4.494138	0.035925
HBAT	HBQ1	Hemoglobin subunit theta-1	4.128817	0.031052

BML, benign mass-like; BNML, benign non-mass-like; FC, fold change.

Table 6 Some down-regulated proteins in BML/BNML

ID	Gene name	Description	FC	P value
PTH	PTRH1	Probable peptidyl-tRNA hydrolase	0.121963	0.031824
HMCS2	HMGCS2	Hydroxymethylglutaryl-CoA synthase, mitochondrial	0.127029	0.046378
MUCL1	MUCL1	Mucin-like protein 1	0.128836	0.048632
PNMT	PNMT	Phenylethanolamine N-methyltransferase	0.199291	0.041889
SULF2	SULF2	Extracellular sulfatase Sulf-2	0.230463	0.03582
PRC2C	PRRC2C	Protein PRRC2C	0.235124	0.027068
YTDC1	YTHDC1	YTH domain-containing protein 1	0.244612	0.031507
GPKOW	GPKOW	G-patch domain and KOW motifs-containing protein	0.249811	0.040969
RPC4	POLR3D	DNA-directed RNA polymerase III subunit RPC4	0.255658	0.024292
PLCC	AGPAT3	1-acyl-sn-glycerol-3-phosphate acyltransferase gamma	0.258439	0.008054

BML, benign mass-like; BNML, benign non-mass-like; FC, fold change.

of the top 10 differentially expressed key proteins in the MML/MNML and BML/BNML groups were shown in *Figure 4A* and *Figure 4B*.

Discussion

ML and NML are US morphological types of breast diseases. Previous studies have shown that the formation of ML and NML may be related to nutritional status, invasiveness, and other factors (10,11). However, many molecular participants and mechanisms behind the morphological formation of US images are still unclear.

The progress of biomedical research is expected to uncover new molecular discoveries of ML and NML breast lesions. Clinical proteomics is currently undergoing rapid advances in technologies that are expected to provide new means of improving the early diagnosis, stratification, and treatment response to breast lesions. In this study, DIA-based quantitative proteomics was applied to study the histological reasons for the morphological differences between NML and ML, so as to explore the formation mechanism of ML or NML that may affect the ultrasonic morphology of breast lesions. Numerous significantly differentially expressed proteins were identified between the MML/
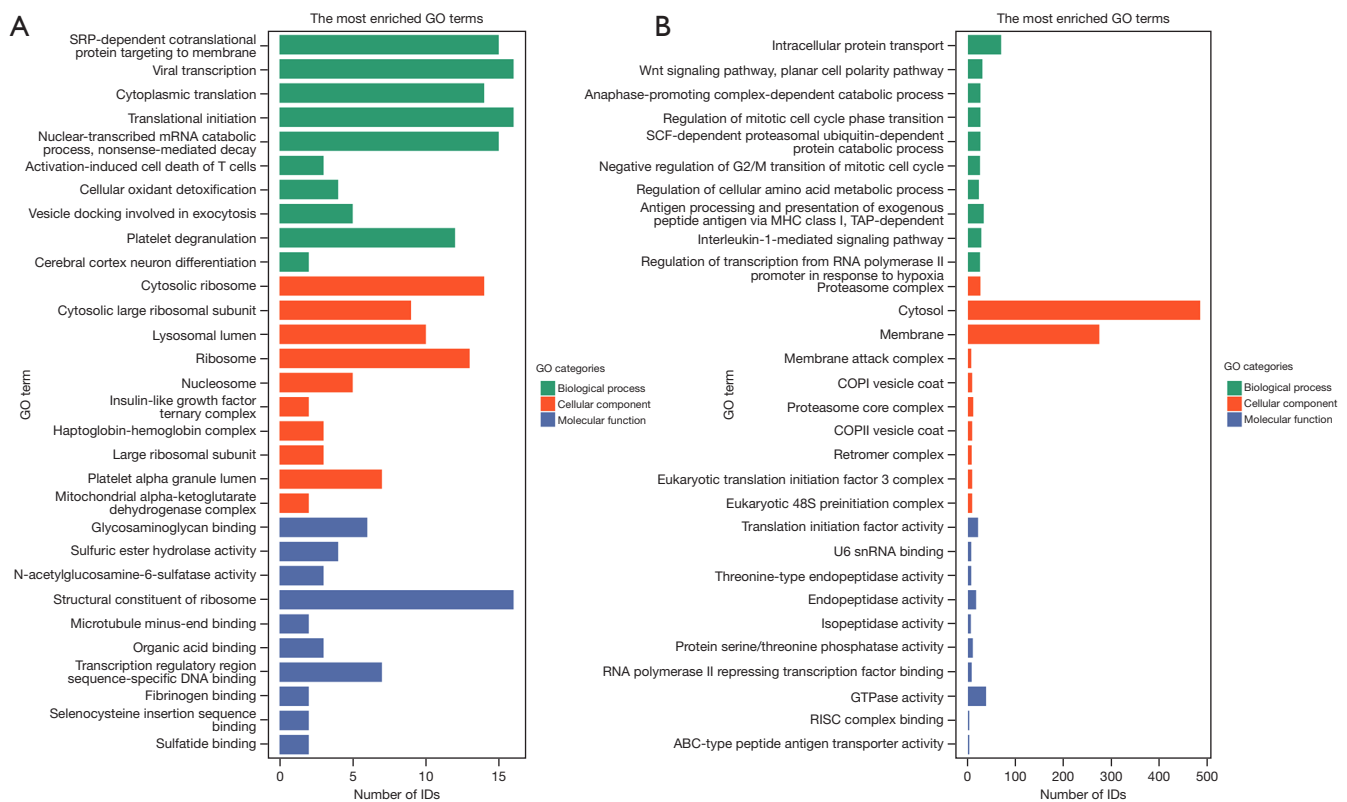
Page 8 of 12

Li et al. Proteomic comparison of breast ML and NML lesions

Figure 2 The GO analyses results of the MML/MNML group (A) and the BML/BNML group (B). GO, Gene Ontology; MML, malignant mass-like; MNML, malignant non-mass-like; BML, benign mass-like; BNML, benign non-mass-like.

MNML and BML/BNML groups.

DIA proteomics was performed in 20 cases of ML and NML breast cancers and 17 cases of ML and NML benign lesions. The results showed that 623 and 167 proteins were significantly different in MML/MNML and BML/BNML groups, respectively (P<0.05). Previous studies have shown that there are significant differences in the biomarkers between MML and MNML (10,11). To further explore the functions of the differential proteins, GO, KEGG, and PPI analyses were performed on the MML/MNML and BML/BNML groups, respectively.

The TNF signaling pathway is involved in the immune response of several protein families and plays a key role in innate and acquired immunity (20,21). TNF-α has been found to induce epithelial-mesenchymal transformation (EMT) in multiple breast cancer cell lines, transforming cells into mesenchymal cell phenotypes and increasing the number of stem cells (22). It has also been found to induce EMT in several breast cancer cell lines, leading to the transformation of cells to the mesenchymal cell phenotype and an increased number of stem cells (22). In

this study, it was shown that in the MML/MNML group, the up-regulated differential proteins of the TNF signaling pathway were enriched in both the MML/MNML and BML/BNML groups, suggesting that the TNF signaling pathway may be related to the ultrasonic morphological changes of breast lesions. In the MML/MNML group, the KS6A5, NFKB1, CASP3, MK09, MP2K4, MP2K3, MP2K6, FADD, CASP8, MLKL, and PGAM5 up-regulated proteins may be involved in biological processes such as apoptosis, necroptosis, intracellular signal transduction, and cell degeneration of MML. In the BML/BNML group, the MMP9, TNR6, and MP2K3 differential proteins were up-regulated in the TNF signaling pathway, suggesting that MMP9, TNR6, and MP2K3 may be involved in BML intracellular signal transduction and cell survival and other biological processes.

The DIA results in this study showed that MP2K3 protein expression was significantly up-regulated in the TNF signaling pathway of the MML/MNML and BML/BNML groups, suggesting that MP2K3 may be related to the formation of the ultrasonic morphology of breast
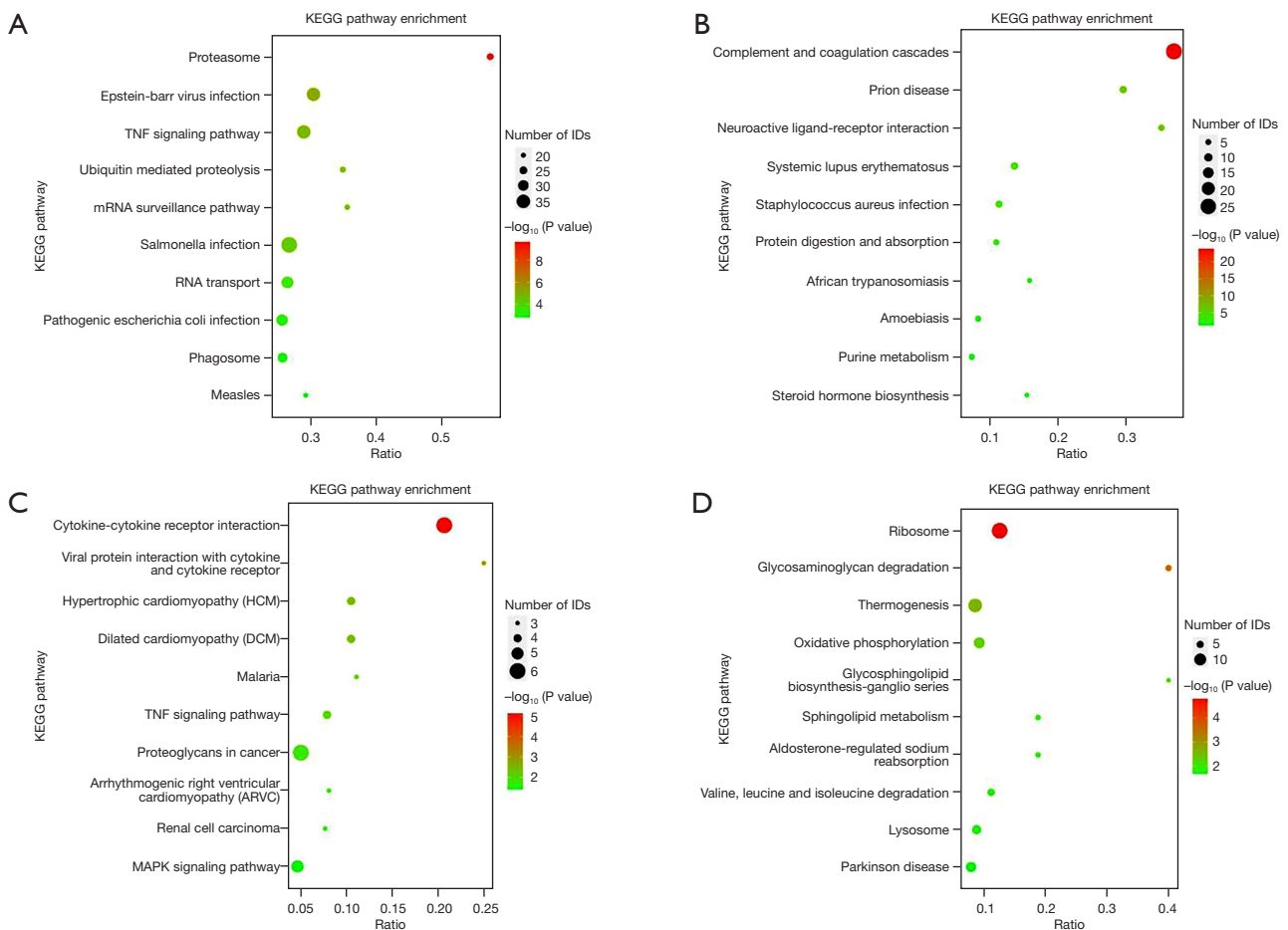
Figure 3 The top 10 up-and down-regulated protein enrichment KEGG pathways in the MML/MNML (A,B) and BML/BNML (C,D) groups. KEGG, Kyoto Encyclopedia of Genes and Genomes; TNF, tumor necrosis factor; MML, malignant mass-like; MNML, malignant non-mass-like; BML, benign mass-like; BNML, benign non-mass-like.
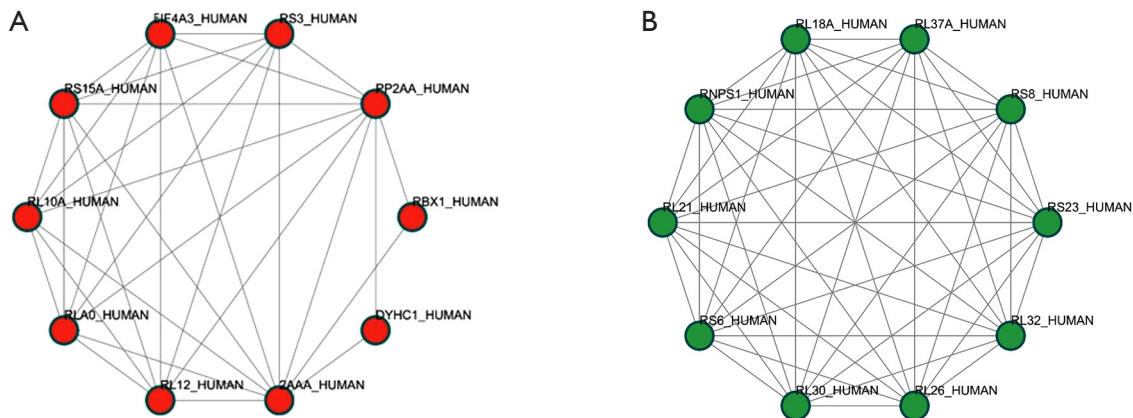

Figure 4 The specific linkage results of the top 10 key proteins in the PPI network in the MML/MNML (A) and the BML/BNML (B) groups. PPI, protein-protein interaction; MML, malignant mass-like; MNML, malignant non-mass-like; BML, benign mass-like; BNML, benign non-mass-like.

lesions. MP2K3 is a bispecific kinase belonging to the MAP kinase family. It is activated by inflammation and endoplasmic reticulum stress, phosphorylates and activates the 38 mitogen-activated protein kinase axis, and participates in cell growth, differentiation, apoptosis, movement, and inflammation (23). In addition, studies have shown that MP2K3 may also be involved in the EMT of primary tumor cells (24,25). Peng *et al.* (25) confirmed that MP2K3 knockout can inhibit the growth, proliferation, invasion, and migration of cervical cancer *in vitro* and *in vivo*. Xie *et al.* (26) used MP2K3 inhibitors to inhibit esophageal cancer *in vitro* and *in vivo*. Jia *et al.* (27) found that MP2K3 has pro-aging activity and is down-regulated in human breast cancer compared with normal human mammary epithelial cells. In the breast cancer model of MacNeil *et al.* (28), activated MP2K3 significantly limited tumor growth *in vivo* and *in vitro* cell line expression systems, while impaired MP2K3 signaling significantly promoted tumor growth. In this study, the expression of MP2K3 was not only up-regulated in MML compared to MNML but was also up-regulated in BML relative to BNML, suggesting that MP2K3 may be related to the ultrasonic morphology of breast lesions.

We also analyzed the functions of proteins with significant expression differences in the MML/MNML group, screened out some interesting proteins that may have important clinical significance, and preliminarily explored their possible mechanisms in the formation of MML. The expressions of EIF4A3, 2AAA, RPS3, PP2AA, DYNC1H1, TGF-β1, TSP1, IGF1, and ITGB5 protein in MML was higher than that in MNML, suggesting that these proteins may be related to the ultrasonic morphological characteristics of breast cancer. Thus, further exploration of the specific mechanism of these proteins in the formation of MML and MNML ultrasonic morphology is needed.

This study still has some limitations that should be noted. Firstly, this study compared the proteomic differences between mass and non-mass breast lesions; however, the sample size was not sufficient, and the proteomic results need to be further verified. Second, as a prospective study, there are still some pathological types that were not involved. Moreover, the selection of breast lesions was closely related to the experience of the operator, and the different parts of the same lesion were related to the final diagnosis results, with a certain degree of subjectivity. Besides, our study lacked further validation of MP2K3 and TNF signaling pathways. In the following studies, we intend to further verify this with western blot.

In addition, in the next research, we can also add studies on the correlation between breast cancer histopathological factors and TNF signaling pathway and MP2K3.

Conclusions

Our results illustrated that the TNF signaling pathway may be related to the ultrasonic morphological characteristics of breast lesions. MP2K3 is an up-regulated differentially expressed protein in the MML/MNML and BML/BNML groups, which may be related to the ultrasonic morphological characteristics of breast lesions. However, further studies are needed to explore the underlying biological mechanisms of MP2K3 and TNF signaling in the US morphology of breast lesions.

Acknowledgments

Footnote

References

1. Barzaman K, Karami J, Zarei Z, et al. Breast cancer: Biology, biomarkers, and treatments. Int Immunopharmacol 2020;84:106535.

2. Sung H, Ferlay J, Siegel RL, et al. Global Cancer Statistics 2020: GLOBOCAN Estimates of Incidence and Mortality Worldwide for 36 Cancers in 185 Countries. CA Cancer J Clin 2021;71:209-49.

3. Li T, Mello-Thoms C, Brennan PC. Descriptive epidemiology of breast cancer in China: incidence, mortality, survival and prevalence. Breast Cancer Res Treat 2016;159:395-406.

4. Brem RF, Lenihan MJ, Lieberman J, et al. Screening breast ultrasound: past, present, and future. AJR Am J Roentgenol 2015;204:234-40.

5. Wang ZL, Li N, Li M, et al. Non-mass-like lesions on breast ultrasound: classification and correlation with histology. Radiol Med 2015;120:905-10.

6. Wang ZL, Li Y, Wan WB, et al. Shear-Wave Elastography: Could it be Helpful for the Diagnosis of Non-Mass-Like Breast Lesions? Ultrasound Med Biol 2017;43:83-90.

7. Zhang W, Xiao X, Xu X, et al. Non-Mass Breast Lesions on Ultrasound: Feature Exploration and Multimode Ultrasonic Diagnosis. Ultrasound Med Biol 2018;44:1703-11.

8. Li J, Yuan M, Yang L, et al. Correlation of contrast-enhanced ultrasound features with prognostic factors in invasive ductal carcinomas of the breast. Jpn J Radiol 2020;38:960-7.

9. Kim KE, Park H, Bae SH, et al. Usefulness of using additional ultrasonic dissection device in breast cancer surgery: a retrospective cohort study. Gland Surg 2021;10:3181-7.

10. Morishima I, Ueno E, Tohno E, et al. Ultrasonic diagnosis of non-mass image-forming breast cancer. In: Ueno E, Shiina T, Kubota M, et al. editors. Research and Development in Breast Ultrasound. Tokyo, Japan: Springer, 2005:127-34.

11. Franks SJ, Byrne HM, Mudhar HS, et al. Mathematical modelling of comedo ductal carcinoma in situ of the breast. Math Med Biol 2003;20:277-308.

12. Ko KH, Jung HK, Kim SJ, et al. Potential role of shear-wave ultrasound elastography for the differential diagnosis of breast non-mass lesions: preliminary report. Eur Radiol 2014;24:305-11.

13. Jiang L, Zhou Y, Wang Z, et al. Is there different correlation with prognostic factors between "non-mass" and "mass" type invasive ductal breast cancers? Eur J Radiol 2013;82:1404-9.

14. Neagu AN, Whitham D, Buonanno E, et al. Proteomics and its applications in breast cancer. Am J Cancer Res 2021;11:4006-49.

15. Hu A, Noble WS, Wolf-Yadlin A. Technical advances in proteomics: new developments in data-independent acquisition. F1000Res 2016;5:eF1000 Faculty Rev-419.

16. Lin Y, Lin L, Fu F, et al. Quantitative proteomics reveals stage-specific protein regulation of triple negative breast cancer. Breast Cancer Res Treat 2021;185:39-52.

17. Wang R, Yin Y, Zhu ZJ. Advancing untargeted metabolomics using data-independent acquisition mass spectrometry technology. Anal Bioanal Chem 2019;411:4349-57.

18. Chae YK, Gonzalez-Angulo AM. Implications of functional proteomics in breast cancer. Oncologist 2014;19:328-35.

19. Yanovich G, Agmon H, Harel M, et al. Clinical Proteomics of Breast Cancer Reveals a Novel Layer of Breast Cancer Classification. Cancer Res 2018;78:6001-10.

20. Stöhr D, Jeltsch A, Rehm M. TRAIL receptor signaling: From the basics of canonical signal transduction toward its entanglement with ER stress and the unfolded protein response. Int Rev Cell Mol Biol 2020;351:57-99.

21. Park YH, Jeong MS, Jang SB. Structural insights of homotypic interaction domains in the ligand-receptor signal transduction of tumor necrosis factor (TNF). BMB Rep 2016;49:159-66.

22. Bhatt AB, Patel S, Matossian MD, et al. Molecular Mechanisms of Epithelial to Mesenchymal Transition Regulated by ERK5 Signaling. Biomolecules 2021;11:183.

23. Kanda T, Sasaki-Tanaka R, Masuzaki R, et al. Knockdown of Mitogen-Activated Protein Kinase Kinase 3 Negatively Regulates Hepatitis A Virus Replication. Int J Mol Sci 2021;22:7420.

24. Bhowmick NA, Zent R, Ghiassi M, et al. Integrin beta 1 signaling is necessary for transforming growth factor-beta

Page 12 of 12

Li et al. Proteomic comparison of breast ML and NML lesions

activation of p38MAPK and epithelial plasticity. J Biol Chem 2001;276:46707-13.

25. Peng R, Cheng X, Zhang Y, et al. miR-214 down-regulates MKK3 and suppresses malignant phenotypes of cervical cancer cells. Gene 2020;724:144146.

26. Xie X, Liu K, Liu F, et al. Gossypetin is a novel MKK3 and MKK6 inhibitor that suppresses esophageal cancer growth in vitro and in vivo. Cancer Lett 2019;442:126-36.

27. Jia M, Souchelnytskyi N, Hellman U, et al. Proteome profiling of immortalization-to-senescence transition of human breast epithelial cells identified MP2K3 as a senescence-promoting protein which is downregulated in human breast cancer. Proteomics Clin Appl 2010;4:816-28.

28. MacNeil AJ, Jiao SC, McEachern LA, et al. MAPK kinase 3 is a tumor suppressor with reduced copy number in breast cancer. Cancer Res 2014;74:162-72.

(English Language Editor: A. Kassem)